Atmos. Chem. Phys. Discuss., doi:10.5194/acp-2016-922, 2016
Manuscript under review for journal Atmos. Chem. Phys.
Published: 29 November 2016

Atmospheric Chemistry and Physics Discussions

The impact of fluctuations and correlations in droplet growth by collision-coalescence revisited. Part I: Numerical calculation of post-gel droplet size distribution

Lester Alfonso[1], Graciela B. Raga[2]

[1]Universidad Autónoma de la Ciudad de México, México City, 09790 México

[2]Centro de Ciencias de la Atmósfera, UNAM, México City, 04510 México

Correspondence to: Lester Alfonso (lesterson@yahoo.com)

Abstract. The impact of stochastic fluctuations in cloud droplet growth is a matter of broad interest, since stochastic effects are one of the possible explanations of how cloud droplets cross the size-gap and form the raindrop embryos that trigger warm rain development in cumulus clouds. Most theoretical studies in this topic rely on the use of the kinetic collection equation, or the Gillespie stochastic simulation algorithm. However, the kinetic collection equation is a deterministic equation with no stochastic fluctuations. Moreover, the traditional calculations using the kinetic collection equation are not valid when the system undergoes a transition from a continuous distribution to a distribution plus a runaway raindrop embryo (known as the sol-gel transition). On the other hand, the stochastic simulation algorithm, although intrinsically stochastic, fails to reproduce adequately the large end of the droplet size distribution due to the huge number of realizations required. Therefore, the full stochastic description of cloud droplet growth must be obtained from the solution of the master equation for stochastic coalescence.

Atmos. Chem. Phys. Discuss., doi:10.5194/acp-2016-922, 2016
Manuscript under review for journal Atmos. Chem. Phys.
Published: 29 November 2016

Atmospheric Chemistry and Physics Discussions

In this study the master equation is used to calculate the evolution of the droplet size distribution after the sol-gel transition. These calculations show that after the formation of the raindrop embryo, the expected droplet mass distribution strongly differs from the results obtained with the kinetic collection equation. Furthermore, the low mass bins and bins from the gel fraction are strongly anti-correlated in the vicinity of the critical time, this being one of the possible explanations for the differences between the kinetic and stochastic approaches after the sol-gel transition. Calculations performed within the stochastic framework provide insight into the inability of explicit microphysics cloud models to explain the droplet spectral broadening observed in small, warm clouds.

Atmos. Chem. Phys. Discuss., doi:10.5194/acp-2016-922, 2016
Manuscript under review for journal Atmos. Chem. Phys.
Published: 29 November 2016

Atmospheric Chemistry and Physics Discussions

1. **Introduction**

Although rain has been observed to form in warm cumulus clouds within about twenty minutes, calculations that represent condensation and coalescence accurately in such clouds have had difficulty producing rainfall in such a short time except via processes involving giant cloud condensation nuclei (with diameters larger than 2 μm). One of the possible origins of this discrepancy is the stochastic nature of the collision coalescence process that is not well reflected in current models that rely almost exclusively in the kinetic collection (or Smoluchowski) equation, hereafter referred to as KCE (Pruppacher and Klett, 1997):

$$\frac{\partial N(i,t)}{\partial t} = \frac{1}{2}\sum_{j=1}^{i-1} K(i-j,j)N(i-j)N(j) - N(i)\sum_{j=1}^{\infty} K(i,j)N(j) \quad (1)$$

where $N(i,t)$ is the concentration of droplets in bin i and $K(i,j)$ is the collection kernel for droplets in bins i and j. Additionally, Eq. (1) fails to represent the droplet size distribution at the time when raindrop embryos are formed (Alfonso et al., 2008), as there is a transition from a continuous distribution to a continuous distribution *plus* a massive raindrop embryo (i.e, the "runaway droplet"). At that point, the infinite system exhibits a sol-gel transition (also called gelation and in which the "runaway droplet" is labeled "gel"), the KCE breaks down and the total mass of the system calculated according to the KCE is no longer conserved.

One way to avoid this problem is to adopt the stochastic finite volume description of the coalescence process by using the stochastic simulation algorithm proposed by Gillespie (1975). The stochastic simulation algorithm (hereafter referred as SSA), correctly accounts for fluctuations and correlations, and has been used in cloud simulation studies with realistic collection kernels (Valioulis and List, 1984).

Atmos. Chem. Phys. Discuss., doi:10.5194/acp-2016-922, 2016
Manuscript under review for journal Atmos. Chem. Phys.
Published: 29 November 2016

Atmospheric Chemistry and Physics Discussions

However, the SSA has difficulties in accurately reproducing the large end of the droplet size distribution. This is due to the huge number of realizations required to obtain a smooth behaviour at the large end of the droplet size distribution (Alfonso, 2015). The alternative approach (within the stochastic framework) is to use the master equation:

$$\frac{\partial P(\bar{n})}{\partial t} = \sum_{i=1}^{N}\sum_{j=i+1}^{N} K(i,j)(n_i+1)(n_j+1)P(\ldots,n_i+1,\ldots,n_j+1,\ldots,n_{i+j}-1,\ldots;t)$$
$$+\sum_{i=1}^{N}\frac{1}{2}K(i,i)(n_i+2)(n_i+1)P(\ldots,n_i+2,\ldots,n_{2i}-1,\ldots;t)$$
$$-\sum_{i=1}^{N}\sum_{j=i+1}^{N} K(i,j)n_i n_j P(\bar{n};t) - \sum_{i=1}^{N}\frac{1}{2}K(i,i)n_i(n_i-1)P(\bar{n};t) \qquad (2)$$

The master equation (2) is a gain-loss equation for the probability of each state $P(\bar{n})$. The sum of the first two terms is the gain due to transition from other states, and the sum of the last two terms is the loss due to transitions into other states. This formulation was introduced in the pioneer works of Marcus (1968) and Bayewitz et al. (1974), and was studied in detailed by Lushnikov (1978, 2004) and Tanaka and Nakazawa (1993). However, these studies only offer analytical results for a limited number of cases (with constant, sum and product kernels), for mono-disperse initial conditions. Furthermore, most of these studies are limited to non-gelling conditions and do not provide a coherent framework for the general case.

The exception are the methods developed by Lushnikov (2004) from the analytical solution of the master equation, and more recently by Matsoukas (2015), the later based on arguments from statistical physics. These methods, although also limited to very special cases (product kernel and mono-disperse initial conditions), are capable of obtaining solutions in the post-gel regime. For example, in Lushnikov (1978,

Atmos. Chem. Phys. Discuss., doi:10.5194/acp-2016-922, 2016
Manuscript under review for journal Atmos. Chem. Phys.
Published: 29 November 2016

2004), the coalescence process takes place in a system with a finite volume that includes a finite number of particles. Within this approach any losses of mass are, by definition, excluded. In the infinite system described by the KCE (Eq. 1), the coagulation process instantly transfers mass to the gel, while in the finite system the gel coalesces with smaller particles decreasing their concentration not instantly by rather in a finite time.

In order to study the droplet size distribution after the formation of raindrop embryos (sol-gel transition), for systems with kernels relevant to cloud physics and arbitrary initial conditions, we must rely on numerical methods capable of solving the master equation (Eq. 2). We can address this problem through a detailed comparison of the droplet size distributions obtained from the stochastic description for a finite system with the master equation (Eq. 2), and the deterministic approach for an infinite system by using the KCE (Eq. 1), using the numerical algorithm reported in Alfonso (2015). By the time the gel forms, certain differences are to be expected between the two approaches at the large end of the droplet size distribution.

This analysis of the sol-gel transition problem in the cloud physics context could provide an alternative explanation of the differences between modeled and observed droplet spectra in clouds. Several mechanisms have been proposed in the past (entrainment, presence of giant nuclei, supersaturation fluctuations, effects of air turbulence in concentration fluctuations and collision efficiencies, effects of film forming compounds on droplet growth), and a large amount of literature exists regarding the variety of mechanisms that may explain this disparity, but a conclusive answer is still absent. This study does not attempt to dispute any of the mechanisms already proposed, but to explore another mechanism that has not yet been widely considered in the mainstream literature.

Atmos. Chem. Phys. Discuss., doi:10.5194/acp-2016-922, 2016
Manuscript under review for journal Atmos. Chem. Phys.
Published: 29 November 2016

Atmospheric Chemistry and Physics Discussions

The paper is organized as follow: Section 2 presents an overview of the numerical algorithm (following Alfonso, 2015). Numerical results (for the product and hydrodynamic kernels, respectively) with a detailed analysis of the method for calculating the sol-gel transition time, and a comparison with averages calculated with the KCE are presented in Sections 3 and 4. Finally, Section 5 presents a discussion of the limits of applicability of the KCE, an example of correlations in the critical region and conclusions.

2. Overview of previous results: Numerical solution of the master equation.

The algorithm for the numerical solution of the master equation is described in detail in Alfonso (2015), and only a brief summary is presented here. The main idea of the method consists in the numerical calculation of all states for a given initial configuration with probability $P(n_{01}, n_{02}, ..., n_{0N}; 0) = 1$, and the subsequent calculation of the temporal evolution of each state. The time evolution can be performed by considering that the only allowed transitions are of the form: $\bar{n}_1^{(+)} \rightarrow \bar{n}_1$ if $i \neq j$ and $\bar{n}_2^{(+)} \rightarrow \bar{n}_2$ if $i = j$, where $\bar{n}_1^{(+)}$, $\bar{n}_1$ and $\bar{n}_2^{(+)}$, $\bar{n}_2$ are the state vectors:

$$\bar{n}_1^{(+)} = (n_1, ..., n_i + 1, ..., n_j + 1, ..., n_{i+j} - 1, ..., n_N) \quad (3a)$$

$$\bar{n}_1 = (n_1, ..., n_i, ..., n_j, ..., n_{i+j}, ..., n_N) \quad (3b)$$

$$\bar{n}_2^{(+)} = (n_1, ..., n_i + 2, ..., n_{2i} - 1, ..., n_N) \quad (3c)$$

$$\bar{n}_2 = (n_1, ..., n_i, ..., n_{2i}, ..., n_N) \quad (3d)$$

For a system consisting of *N* monomers at *t=0*, the number of possible configurations increases exponentially and can be approximated from the equation (Hall, 1967):

Atmos. Chem. Phys. Discuss., doi:10.5194/acp-2016-922, 2016
Manuscript under review for journal Atmos. Chem. Phys.
Published: 29 November 2016

Atmospheric Chemistry and Physics Discussions

$$R(N) \approx \frac{1}{4N\sqrt{3}} \exp\left(\pi \left(2N/3\right)^{1/2}\right) \tag{4}$$

For example, $R(50)$=217590 and $R(100)$=190 569 232.

The procedure is illustrated for a system with 5 monomers in the initial state, with the 6 possible configurations generated from the initial state $(5,0,0,0,0)$ displayed in Fig. 1.

In a second step, the probabilities of all generated configurations are updated according to the first order finite difference scheme (Alfonso, 2015):

$$\begin{aligned} P\left(\bar{n};t_0+\Delta t\right) = P\left(\bar{n};t_0\right) \\ + \Delta t \sum_{i=1}^{N} \sum_{j=i+1}^{N} K(i,j)(n_i+1)(n_j+1) \\ \times P(\ldots, n_i+1, \ldots, n_j+1, \ldots, n_{i+j}-1, \ldots; t_0) \\ + \Delta t \sum_{i=1}^{N} \frac{1}{2} K(i,i)(n_i+2)(n_i+1) \\ \times P(\ldots, n_i+2, \ldots, n_{2i}-1, \ldots; t_0) \\ - \Delta t \sum_{i,j=1}^{N} K(i,j) n_i n_j P(\bar{n};t_0) \\ - \Delta t \sum_{i=1}^{N} \frac{1}{2} K(i,i) n_i (n_i-1) P(\bar{n};t_0) \end{aligned} \tag{5}$$

From Eq. (5) should be clear that the state probabilities $P\left(\bar{n};t_0+\Delta t\right)$ at $t=t_0+\Delta t$ will increase if the states from which transitions are allowed, have a non-zero probability at $t = t_0$ (second and third terms in the right-hand size of Eq. (5)), and will decrease due to collisions of particles from the same state at $t = t_0$ (fourth term and fifth terms in the right-hand side of Eq. (5)) if $P(\bar{n};t_0)$ is positive.

The finite difference equation for $P(1,0,0,1,0)$ is presented to illustrate the method. From the generation scheme displayed in Figure 1, note that the only allowed transitions to $(1,0,0,1,0)$ are from the states

Atmos. Chem. Phys. Discuss., doi:10.5194/acp-2016-922, 2016
Manuscript under review for journal Atmos. Chem. Phys.
Published: 29 November 2016

Atmospheric Chemistry and Physics Discussions

$(1,2,0,0,0)$ and $(2,0,1,0,0)$. Consequently, at $t=t_0+\Delta t$, $P(1,0,0,1,0;t_0+\Delta t)$ will increase if $P(1,2,0,0,0;t_0)$ and $P(2,0,1,0,0;t_0)$ are positive at $t = t_0$. On the other hand, $P(1,0,0,1,0;t_0+\Delta t)$ will decrease due to collisions from particles within the same state at $t = t_0$ if $P(1,0,0,1,0;t_0)$ is positive. Then, $P(1,0,0,1,0;t_0+\Delta t)$ is calculated from the equation:

$$\begin{aligned} P(1,0,0,1,0;t_0+\Delta t) = P(1,0,0,1,0;t_0) \\ + \Delta t(1/2)K(2,2)(n_2+2)(n_2+1)P(1,2,0,0,0;t_0) \\ + \Delta t K(1,3)(n_1+1)(n_3+1)P(2,0,1,0,0;t_0) \\ - \Delta t K(1,4)(n_1)(n_4)P(1,0,0,1,0;t_0) \end{aligned} \quad (6)$$

The time evolution of the probability of each state was calculated for the product kernel $K(i,j)=Cx_ix_j$, considering C= 5.49x10^{10} cm^3 g^{-2} s^{-1} following Long (1974) and for the initial condition $P(5,0,0,0,0;0)=1$. Due to the small number of droplets in the initial configuration (only 5), the simulated volume was set equal to 10^{-2} cm^3, with an initial droplet radius of 17μm. The time step was Δt=0.1 sec. For this case, the time evolution of four of the seven configurations is displayed in Fig. 2.

After the calculation for each state is completed, the expected values for each droplet mass can be found from the relation (Alfonso, 2015):

$$\langle n_m \rangle = \sum_n nP(n,m;t) \quad (7)$$

where the discrete probability mass function is calculated from the state probabilities following the expression:

$$P(n,m;t) = \sum_{All\ \ states\ \ with\ \ n_m=n} P(n_1,n_2,...,n_m=n,...n_N;t) \quad (8)$$

Atmos. Chem. Phys. Discuss., doi:10.5194/acp-2016-922, 2016
Manuscript under review for journal Atmos. Chem. Phys.
Published: 29 November 2016

Atmospheric Chemistry and Physics Discussions

The expected values $\langle n_m \rangle$ calculated from (Eq. 7) are the magnitudes that must be compared with the averages $N(m;t)$ obtained from the KCE (Eq. 1).

3. Results for the multiplicative kernel

3.1 Estimating the time of gel formation

Lushnikov (2004) demonstrated that right after the sol-gel transition, the particle mass distribution splits into two parts: the thermodynamically-populated one whose behavior is described by the kinetic collection equation, and a narrow peak with a mass very close to the gel mass. For the infinite system described by the kinetic collection equation (Eq. 1) with kernel $K(i,j)=Cx_ix_j$, the critical time is calculated when the second moment of the distribution diverges:

$$M_2(\tau) = \frac{M_2(t_0)}{1 - CM_2(t_0)\tau} \tag{9}$$

leading to the critical time of the sol-gel transition:

$$T_{gel} = \left[CM_2(t_0)\right]^{-1} \tag{10}$$

After $\boldsymbol{\tau} = T_{gel}$ the second moment becomes undefined, and the total mass of the system starts to decrease.

For a finite system, the standard deviation (σ) of the mass of the largest droplet is an important quantity in order to calculate the critical time of the gel formation (Botet, 2011). At the critical time for the infinite system σ must diverge, since it is proportional to the second moment of the distribution $M_2(\tau)$ which diverges at the gelation point. However, for a finite system (with no critical behavior), the standard

Atmos. Chem. Phys. Discuss., doi:10.5194/acp-2016-922, 2016
Manuscript under review for journal Atmos. Chem. Phys.
Published: 29 November 2016

Atmospheric Chemistry and Physics Discussions

deviation of the mass of the largest droplet $\sigma(S_{\max})$ is expected to reach a maximum for a time close to $T_{gel} = [CM_2(t_0)]^{-1}$.

This was explored in previous studies (Inaba, 1999; Alfonso et al., 2008, 2010, 2013), where σ was calculated for a finite system from Monte Carlo simulations in order to estimate the sol-gel transition times for the corresponding deterministic model of an infinite system. We can perform an example calculation of σ by using the species formulation of the SSA (Laurenzi and Diamond, 2002), in this case:

$$\sigma(S_{\max}) = \sqrt{\frac{1}{N_r}\sum_{i=1}^{N_r}(S^i_{\max} - \langle S_{\max}\rangle)^2} \qquad (11)$$

where S^i_{max} is the value of $S_{\max} = M_{\max}/\langle M_{\max}\rangle$ for each realization at a given time, and N_r is the number of iterations of the SSA, $M_{\max}$ the size of the largest particle, and $\langle M_{\max}\rangle$ its ensemble mean over all the realizations. The time evolution of $\sigma(S_{\max})$ is shown in Figure 3 for a finite system with N=40 droplets of 17 μm in radius (droplet mass = 2.058×10^{-8}g) in a volume of 1 cm^3. For the product kernel with C= $5.49\text{x}10^{10}$ cm^3 g^{-2} s^{-1}, the maximum occurs at T=1065 s, which is close to the sol-gel transition time T_{gel}=1075 s.

3.2 Calculation of the post-gel droplet size distribution from the master equation and comparison with the deterministic (kinetic) approach

The evolution of a system with an initial mono-disperse droplet size distribution of N_0=40 droplets of 17 μm in radius at t_0, in a volume of $1cm^3$, and a corresponding liquid water content (LWC) of 0.823 gm^{-3}, was calculated using the master equation (Eq. 2). The initial condition for this case is $P(40,0,...,0;0)=1$

Atmos. Chem. Phys. Discuss., doi:10.5194/acp-2016-922, 2016
Manuscript under review for journal Atmos. Chem. Phys.
Published: 29 November 2016

Atmospheric Chemistry and Physics Discussions

and the time step was set equal to Δt=0.1s. The results for the droplet mass distribution are displayed in Figure 4 at t=300, 1000, 1800 and 2200s. Note that the gel is clearly seen in the distributions at 1800 and 2200s but not at 1000s.

To proceed further, the previous results are compared against the analytical size distributions from the KCE (Eq.1) calculated for the product kernel with mono-disperse initial conditions before (t=300s) and after (t=1200s) gel formation (Laurenzi and Diamond, 2002):

$$N(i,t) = N_0 \frac{(iT)^{i-1}}{i\Gamma(i+1)} \exp(-iT) \qquad \text{where} \qquad T = CN_0 v_0^{\,2} t \tag{12}$$

In Eq. (12), N_0=40 is the initial concentration and v_0 is the initial volume of droplets. The index i represents the bin size and C= 5.49x10^{10} cm^3 g^{-2} s^{-1}.

The comparison of the droplet mass concentration ($g_{KCE}(m) = N(m,t)m$) calculated from Eq. 12, with expected values ($g_{STOC}(m) = \langle n_m \rangle m$) calculated from the master equation (Eq. 2) with the same initial conditions are displayed in Figure 5 at t=300, 1200s. Note that the KCE fails to capture the gel formation after the critical time, and the droplet mass concentration calculated using the kinetic approach is much lower at the large end of the distribution. This is due to the fact that the total mass calculated according to Eq. 12 decreases after the sol-gel transition time. This decrease can be clearly seen in the time evolution of the LWC from the kinetic approach using the relation:

$$M_1(t) = \sum_{i=1}^{\infty} m(i) N(i,t) \tag{13}$$

Atmos. Chem. Phys. Discuss., doi:10.5194/acp-2016-922, 2016
Manuscript under review for journal Atmos. Chem. Phys.
Published: 29 November 2016

Atmospheric Chemistry and Physics Discussions

where $m(i)$ is the mass for bin size i. After t~1000s (Figure 6) the total mass of the system calculated according to the KCE starts to decrease, while the total mass calculated from the stochastic approach is conserved at all times.

3.3 Calculation of the gel mass

Within the master equation approach, the expected value of the mass of the largest droplet M_1 is approximately given by (Tanaka and Nakazawa, 1994):

$$M_1 = \sum_{i=i_1}^{N} m(i)\langle n_i \rangle \tag{14}$$

where $\langle n_i \rangle$ are is the expected number for each droplet size values calculated from Eq. (7), $m(i)$ is the mass for bin size i, and the bin number i_1 is defined from the relation:

$$\sum_{i=i_1}^{N} \langle n_i \rangle = 1 \tag{15}$$

The mass of the gel, M_1, is evaluated for t=1200, 1800 and 2200s from Eqs (14) and (15).

Within the Monte Carlo stochastic approach (SSA), the expected mass of the gel is the ensemble mean ($M_{1\text{-}MC}$) calculated over all realizations (N_r) of the mass of the largest droplet (Alfonso et al., 2008):

$$M_{1\_MC} = \frac{1}{N_r} \sum_{i=1}^{N_r} M_1^{\,i} \tag{16}$$

where N_r =1000 for this simulation and M^i_1 is the largest droplet for each realization. The results obtained from both the master equation and the SSA are displayed in Table 1, showing a very good correspondence between the two approaches.

Atmos. Chem. Phys. Discuss., doi:10.5194/acp-2016-922, 2016
Manuscript under review for journal Atmos. Chem. Phys.
Published: 29 November 2016

Atmospheric Chemistry and Physics Discussions

After the sol-gel transition the mass of the gel can also be estimated by using the infinite system approach from the relation (Wetherill, 1990):

$$M_{Gel} = M_0 - M_{KCE} \tag{17}$$

where M_0 the initial is mass of the system, and M_{KCE} is the mass calculated from Eq. (13). The results shown in the third column of Table 1, indicate good agreement away from the sol-gel transition time.

4. Results for the hydrodynamic collection kernel

Collisions between droplets under pure gravity conditions are simulated with the hydrodynamic kernel, which has the following expression:

$$K_g(x_i, x_j) = \pi(r_i + r_j)^2 \left|V(x_i) - V(x_j)\right| E(r_i, r_j) \tag{18}$$

The hydrodynamic kernel takes into account the fact that droplets with different masses (x_i and x_j and corresponding radii, r_i and r_j) have different terminal velocities, which are functions of their masses. In Eq. 18, $E(r_i, r_j)$ are the collection efficiencies calculated according to Hall (1980).

4.1 Estimating the time of gel formation and the gel mass

For an infinite system modeled by the KCE (Eq. 1) with the hydrodynamic kernel, the second moment of the mass distribution (M_2) diverges when the raindrop embryo (gel) forms. As there is no a simple analytical expression to calculate the critical time (see Eq. 9 for the product kernel) in this case, Monte Carlo simulations for the finite system could provide insightful information.

The sol-gel transition time can be estimated approximately by calculating the time when the time series of $\sigma(S_{\max})$ in the SSA exhibits a maximum (Alfonso et al., 2010). As in the case of multiplicative kernel,

Atmos. Chem. Phys. Discuss., doi:10.5194/acp-2016-922, 2016
Manuscript under review for journal Atmos. Chem. Phys.
Published: 29 November 2016

Atmospheric Chemistry and Physics Discussions

the time evolution of $\sigma(S_{max})$ is calculated for a cloud volume of 1 cm^3 with an initial bi-disperse distribution (20 droplets of 17 μm in radius, and 10 droplets of 21.4 μm), and the time evolution of $\sigma(S_{max})$ is calculated from 1000 realizations (N_r=1000) of the SSA. Figure 7 shows that there is a maximum at t=1310s, which is considered a good estimate for the sol-gel transition time for the infinite system. Thus, the distributions obtained from the stochastic (master equation) and the deterministic (kinetic collection equation) approaches must be compared before and after 1310s. After the critical time, the gel mass was calculated using Eqs. (14) and (15). The results are displayed in Table 2, showing, again, a good agreement between the calculations performed with the SSA and the master equation.

4.2 Calculation of the post-gel droplet size distribution from the master equation and comparison with the deterministic (kinetic) approach

The evolution of a system with the initial bi-disperse droplet size distribution described in the previous section is calculated here using the master equation (Eq. 2) with the initial condition $P(20,10,...,0;0)=1$, and a time step Δt=0.1s. The results for the expected droplet mass distribution are displayed in Figure 8 at four different times (t = 500, 1500, 1800 and 2500s).

Before the sol-gel transition, the mass spectrum exponentially decreases with increasing drop radius for both the KCE and the master equation. After the sol-gel transition, there are two behaviors in the droplet mass distribution of the master equation: i) an exponential decay that resembles the KCE description, and ii) a peak in the gel fraction of the distribution, in which the mass is calculated according to Eqs. (14) and (15). As can be observed in Fig. 9, there are substantial differences between the kinetic and the stochastic

Atmos. Chem. Phys. Discuss., doi:10.5194/acp-2016-922, 2016
Manuscript under review for journal Atmos. Chem. Phys.
Published: 29 November 2016

Atmospheric Chemistry and Physics Discussions

approaches especially in the large end of the distribution after the critical time, with much higher values of the droplet mass concentration for the stochastic case.

5. Discussion and conclusions

In their pioneering studies using the stochastic framework, Marcus (1968) and Bayewitz et al. (1974) solved the stochastic master equation (Eq. 2) for a constant collection kernel and a mono-disperse initial droplet distribution. The later study revealed significant deviations from the KCE when there is a small number of droplets in the initial distribution ($\langle N_{Toral} \rangle < 50$). In our work, we extended the results obtained by these authors by calculating the expected droplet size distributions for small systems within the stochastic framework, but by using mass dependent and relevant to cloud physics collection kernels (e.g multiplicative and hydrodynamic). Our results confirm the findings of Bayewitz et al. (1974) that in systems of small populations the results of the kinetic deterministic equations approach may differ substantially from the stochastic means at the large end of the droplet size distribution.

The application of the KCE to coagulating systems also requires that the particles be well-mixed (Bayewitz et al., 1974; Sampson and Ramkrishna, 1985), implying that every pair of droplets is always available for coagulation with each other (Sampson and Ramkrishna, 1985).

Another important assumption is that the droplet population is sufficiently large so that the existence of a droplet with particular properties is not conditionally dependent on the existence or non-existence of any other droplet. In other words, no correlations are assumed in the system, so that $\langle n_i n_j \rangle = \langle n_i \rangle \langle n_j \rangle$.

The assumption that the system is sufficiently large is linked to the fact that the KCE is a deterministic equation that simulates only the mean values and gives an incomplete description of the coagulating

Atmos. Chem. Phys. Discuss., doi:10.5194/acp-2016-922, 2016
Manuscript under review for journal Atmos. Chem. Phys.
Published: 29 November 2016

Atmospheric Chemistry and Physics Discussions

system if fluctuations about the mean are very large (Ramkrishna and Borwanker, 1973). Since fluctuations are proportional to $\sim 1/\sqrt{\langle N_{Total} \rangle}$, a large number of droplets is needed for the fluctuations to be small, and in fact, the larger the number of particles in a system, the smaller the fluctuations. This fact underscores the finite system description adopted in this work, as the collision-coalescence process is limited to pairs of droplets in close proximity to each other. The KCE is not expected to be accurate when the number of droplets or the volume of the system are small.

Additionally, the KCE can fail even if the number of droplets is large when a raindrop embryo forms. At that critical time, there is a transition from a continuous droplet distribution to a continuous distribution *plus* a raindrop embryo (or runaway droplet). This sol-gel transition is well known in other fields (e.g astronomy), but has not been sufficiently explored in the context of cloud physics, where the gel would correspond to the raindrop embryo. This approach is developed in this paper through a detailed comparison of expected values calculated from the stochastic framework with averages obtained from the KCE for realistic collection kernels, before and after the sol-gel transition time.

The marked differences between these two approaches at the sol-gel transition can be related with the increase of correlations at the critical point, and that can happen even for a large number of particles in the initial distribution (Malyshkin and Goldman, 2001). When the sol-gel transition occurs, the occupation numbers n_i of all low-mass bins are strongly anticorrelated with bins from the gel fraction (calculated from Eq. 15). On the other hand, in the vicinity of critical time, the fluctuations for the finite system are larger, since the standard deviation of the mass of the largest droplet, $\sigma(S_{\max})$, has a maximum. In consequence, the differences between the deterministic and stochastic descriptions become larger and divergent. To further analyze this problem, the time evolution of the correlation coefficients

Atmos. Chem. Phys. Discuss., doi:10.5194/acp-2016-922, 2016
Manuscript under review for journal Atmos. Chem. Phys.
Published: 29 November 2016

Atmospheric Chemistry and Physics Discussions

$$\rho_{i,j} = \frac{\mathrm{cov}(n_i, n_j)}{\sqrt{Var(n_i)Var(n_j)}} = \frac{\sigma_{n_i n_j}}{\sigma_{n_i}\sigma_{n_j}} \tag{19}$$

between the random variables n_1 and n_i from bins within the gel fraction (see Eq. 15) were calculated. In the simulations, the gel fraction at *t*=1310s covers the interval bins from 29 to 58 μm, and narrows as time increases. The time evolution of the correlation coefficients for different bin pairs $\rho_{1,20}$, $\rho_{1,25}$, $\rho_{1,30}$, $\rho_{1,35}$ and $\rho_{1,40}$ are displayed in Figure 10, showing in all cases, an increase in the magnitude of the correlation coefficients in the vicinity of the sol-gel transition time. Also in Figure 10, correlations are quite large in magnitude and negative most of the time for $\rho_{1,20}$, $\rho_{1,25}$ and $\rho_{1,30}$ as the mass of the gel increases through coalescence with droplets from low mass bins. However, after 2500s, pairs 1-20, 1-25 and 1-30 are positively correlated as the gel fraction narrows and droplets from bins as large as 20, 25 and 30 are also depleted by the gel. The correlation coefficients for all analyzed pairs have maxima between 1000 and 1500s, in the vicinity of the critical time. The random variable n_{40} is always anticorrelated with n_1, with values much higher than the other pairs after 1500s, and increasing in magnitude until the end of the simulation, which reflects the fact that the gel actively grows by collecting smaller droplets. Thus, for realistic collection kernels, the mean values predicted by the KCE will be not accurate after the sol-gel transition. The stochastic approach captures the gel formation and evolution properly, with larger values of the expected droplet mass at the large end of the distribution.

In principle, this analysis could be performed by using the SSA, which is an alternative tool for the master equation formalism (Eq. 2). However, the number of realizations required to obtain a smooth behavior at the large end in order to compare with averages from the KCE, would be extremely large.

Atmos. Chem. Phys. Discuss., doi:10.5194/acp-2016-922, 2016
Manuscript under review for journal Atmos. Chem. Phys.
Published: 29 November 2016

Atmospheric Chemistry and Physics Discussions

This analysis of the sol-gel transition problem in the cloud physics context, i.e. the formation of a runaway raindrop embryo, provides insight and a possible explanation of the inability of theoretical models to simulate the observed broadening of droplet spectra in small, warm clouds.

Acknowledgements. This study was funded by the grant **"Estancias Sabáticas Nacionales"** from CONACYT, in Mexico and it was completed during an academic visit at Centro de Ciencias de la Atmósfera, UNAM**.** L. Alfonso also thanks the Associate Program of the Abdus Salam International Center of Theoretical Physics (ICTP), in Trieste, for all the support provided for the completion of this paper during the summers of 2015 and 2016.

Atmos. Chem. Phys. Discuss., doi:10.5194/acp-2016-922, 2016
Manuscript under review for journal Atmos. Chem. Phys.
Published: 29 November 2016

Atmospheric Chemistry and Physics Discussions

6. References

Alfonso, L.: An algorithm for the numerical solution of the multivariate master equation for stochastic coalescence. *Atmospheric Chemistry and Physics*, vol. 15, no 21, p. 12315-12326, 2015.

Alfonso, L., Raga and G.B., Baumgardner, D.: The validity of the kinetic collection equation revisited. *Atmos. Chem. Phys.*, 8, 969-982, 2008.

Alfonso, L., Raga, G.B., Baumgardner, D.: The validity of the kinetic collection equation revisited. Part II: Simulations for the hydrodynamic kernel, *Atmos. Chem. Phys.*, 10, 6219-6240, 2010.

Alfonso, L., Raga, G. B., Baumgardner, D.: The validity of the kinetic collection equation revisited–Part 3: Sol–gel transition under turbulent conditions. *Atm ospheric Chemistry and Physics*, vol. 13, no 2, p. 521-529, 2013,

Bayewitz, M.H., Yerushalmi, J., Katz, S., and Shinnar, R.: The extent of correlations in a stochastic coalescence process, *J. Atmos. Sci*., 31, 1604-1614, 1974.

Botet, R.: Where are correlations hidden in the distribution of the largest fragment?. *PoS*, 007, 2011.

Gillespie, D.T.: An Exact Method for Numerically Simulating the Stochastic Coalescence Process in a Cloud, *J. Atmos. Sci*. 32, 1977-1989, 1975.

Hall, M.J.: Combinatorial Theory. Blaisdell Pub. Co., 1967.

Hall, W. D. (1980).: A detailed microphysical model within a two-dimensional dynamic framework: Model description and preliminary results. *Journal of the Atmospheric Sciences*, *37*(11), 2486-2507.

Inaba, S., Tanaka, H., Ohtsuki, K., and Nakazawa, K.: High-accuracy statistical simulation of planetary accretion: I. Test of the accuracy by comparison with the solution to the stochastic coagulation equation, Earth Planet Space, 51, 205-217, 1999.

Laurenzi, I. J., Bartels, J. D., & Diamond, S. L.: A general algorithm for exact simulation of multicomponent aggregation processes. *Journal of Computational Physics*, *177*(2), 418-449, 2002.

Lushnikov, A. A.: Coagulation in finite systems. *Journal of Colloid and Interface Science*, vol. 65, no 2, p. 276- 285, 1978.

Lushnikov, A. A.: From sol to gel exactly. *Physical review letters*, vol. 93, no 19, p. 198302, 2004.

Long, A.B.: Solutions to the droplet collection equation for polynomial kernels, J. Atmos. Sci., 31, 1040-1051, 1974.

Marcus, A. H.: Stochastic coalescence, *Technometrics*, 10.1, 133-143, 1968.

Malyshkin, L., and Goodman, J.: The timescale of runaway stochastic coagulation, *Icarus*, *150*(2), 314-322, 2001.

Matsoukas, Themis.: Statistical Thermodynamics of Irreversible Aggregation: The Sol-Gel Transition. *Scientific reports*, Vol 5, 2015.

Pruppacher, H.R., Klett, J.D.: Microphysics of clouds and precipitation, Kluwer Academic Publishers, 1997.

Ramkrishna, D., & Borwanker, J. D.: A puristic analysis of population balance-I. *Chemical Engineering Science*, *28*(7), 1423-1435,1973.

Sampson, K. J., & Ramkrishna, D.: Particle size correlations and the effects of limited mixing on agglomerating particulate systems. *Journal of colloid and interface science*, *104*(1), 269-276, 1985.

Tanaka, H., Nakazawa, K.: Stochastic coagulation equation and the validity of the statistical coagulation equation, *J. Geomag. Geoelecr*., 45, 361-381, 1993.

Tanaka, H. and Nakazawa, K.: Validity of the statistical coagulation equation and runaway growth of protoplanets. *Icarus*, vol. 107, no 2, p. 404-412, 1994.

Valioulis, I. A. and List, E. J.: A numerical evaluation of the stochastic completeness of the kinetic coagulation equation, J.Atmos. Sci., 41, 2516–2529, 1984.

Wetherill, G.W.: Comparison of analytical and physical modeling of planetesimal Accumulation, *Icarus* 88, 336–354, 1990.

Atmos. Chem. Phys. Discuss., doi:10.5194/acp-2016-922, 2016
Manuscript under review for journal Atmos. Chem. Phys.
Published: 29 November 2016

Atmospheric Chemistry and Physics Discussions

Table 1. Expected gel mass calculated from the SSA, the master equation and the kinetic approach. Simulations were performed for the product kernel.

Time (seconds)	Gel mass (SSA)	Gel mass (Master equation)	Gel mass (KCE)
1200	2.84×10^{-7} g	2.76×10^{-7}g	1.75×10^{-7}g
1800	5.14×10^{-7} g	5.34×10^{-7} g	5.59×10^{-7} g
2200	6.63×10^{-7} g	6.35×10^{-7} g	6.66×10^{-7} g

Atmos. Chem. Phys. Discuss., doi:10.5194/acp-2016-922, 2016
Manuscript under review for journal Atmos. Chem. Phys.
Published: 29 November 2016

Atmospheric Chemistry and Physics Discussions

Table 2. Expected gel mass calculated from the SSA and the master equation. Simulations were performed for the hydrodynamic kernel.

Time (seconds)	Gel mass (SSA)	Gel mass (Master equation)
1200 sec.	1.71×10^{-7} g	1.79×10^{-7}g
1800 sec.	3.34×10^{-7} g	3.37×10^{-7} g
2200 sec.	4.35×10^{-7} g	4.68×10^{-7} g

Atmos. Chem. Phys. Discuss., doi:10.5194/acp-2016-922, 2016
Manuscript under review for journal Atmos. Chem. Phys.
Published: 29 November 2016

Atmospheric Chemistry and Physics Discussions

415

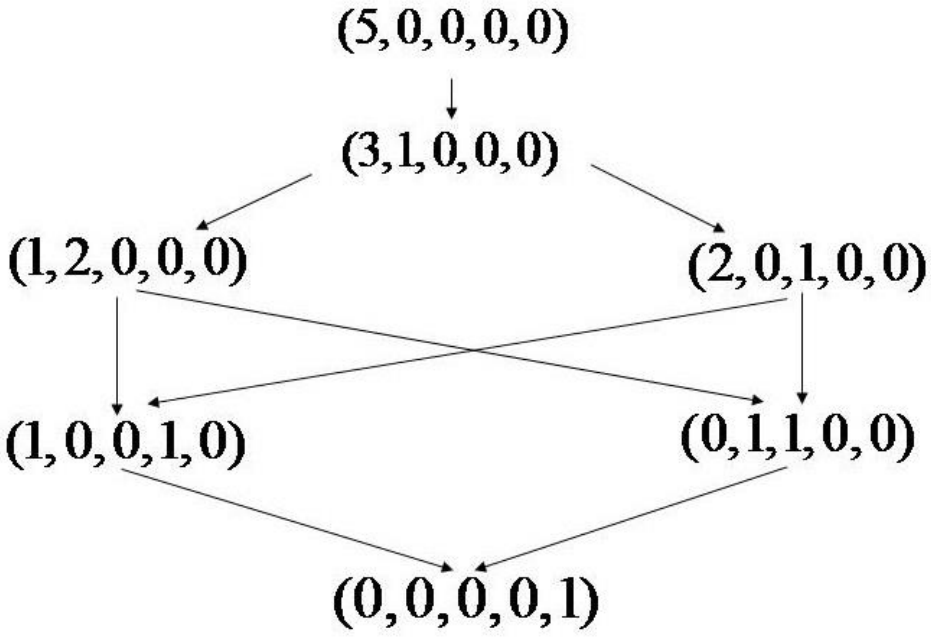

FIG. 1. State space obtained from the initial condition $P(5,0,0,0,0;0)=1$ with the constraint $\sum_{i=1}^{6} in_i = 5$.

420

Atmos. Chem. Phys. Discuss., doi:10.5194/acp-2016-922, 2016
Manuscript under review for journal Atmos. Chem. Phys.
Published: 29 November 2016

Atmospheric Chemistry and Physics Discussions

425

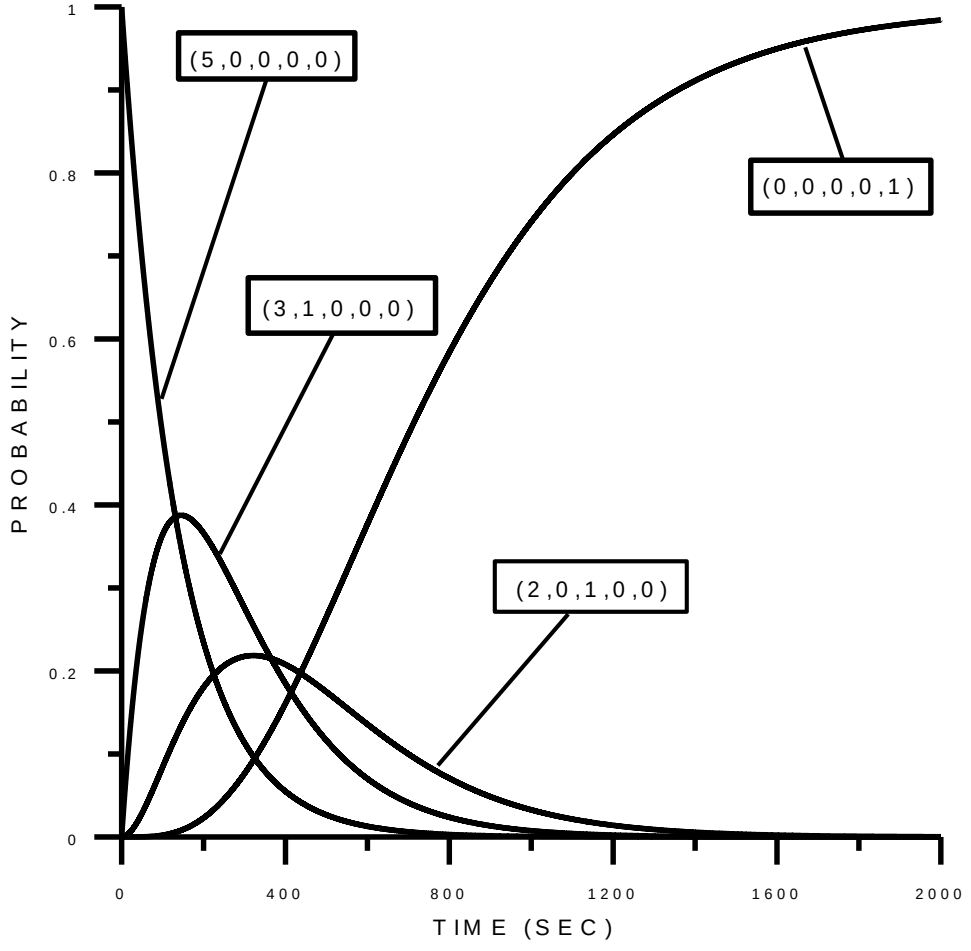

FIG. 2. Time evolution of the probability for 4 of the 7 states for the initial condition $P(5,0,0,0,0;0)=1$. Simulations were performed with the collection kernel $K(i,j)=Cx_ix_j$ (with C= 5.49x10^{10} cm^3 g^{-2} s^{-1}).

430

Atmos. Chem. Phys. Discuss., doi:10.5194/acp-2016-922, 2016
Manuscript under review for journal Atmos. Chem. Phys.
Published: 29 November 2016

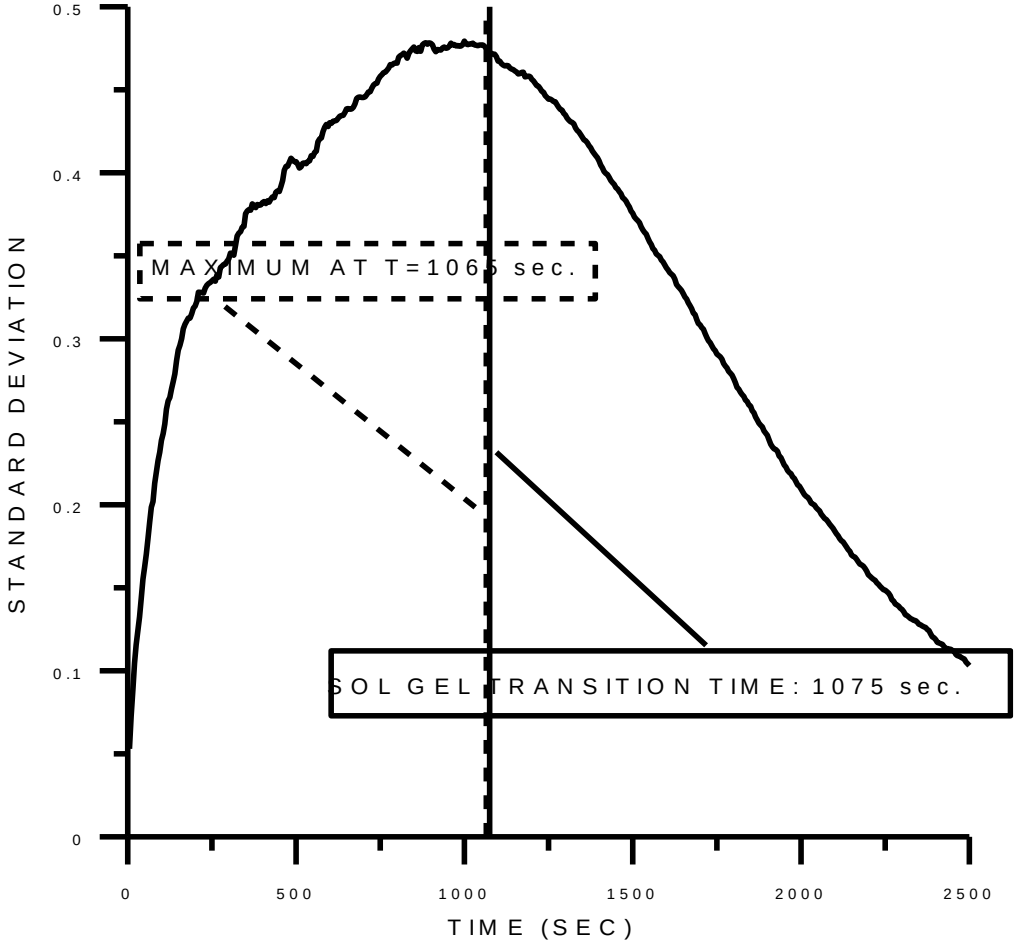

435 FIG 3. For the finite system, standard deviation $\sigma(S_{max})$ of the largest droplet mass versus time. The initial number of droplets was set equal to N=40 droplets of 17 μm in radius in a volume of 1 cm^3. Simulations were performed with the product kernel $K(i,j) = Cx_i x_j$ (with C= 5.49x10^{10} cm^3 g^{-2} s^{-1}), and N_r=2000 realizations of the stochastic algorithm were performed. The maximum value of $\sigma(S_{max})$ is found to be 1065 sec., and is very close to the sol gel transition time for the infinite system (1075 sec.)

440

Atmos. Chem. Phys. Discuss., doi:10.5194/acp-2016-922, 2016
Manuscript under review for journal Atmos. Chem. Phys.
Published: 29 November 2016

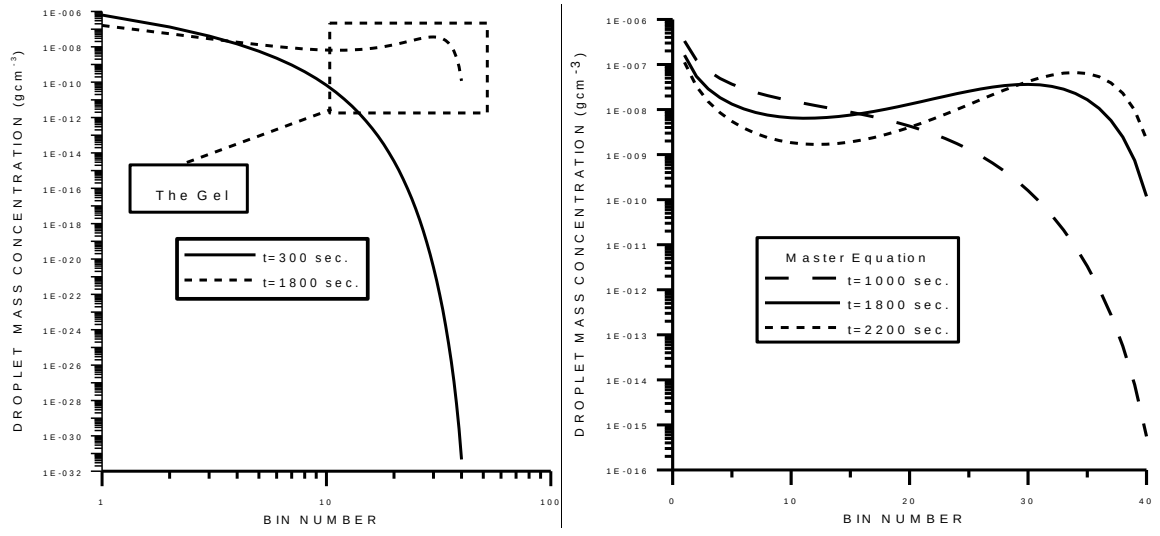

(a) (b)

FIG 4. The droplet mass spectrum at different times (t=300, 1000, 1800 and 2200 sec.). The gel is clearly observed at t=1800, 2200 sec. Simulations were performed with the collection kernel $K(i,j) = Cx_i x_j$ (with C= 5.49x10^{10} cm^3 g^{-2} s^{-1}). The initial number of droplets was set equal to N=40 droplets of 17 μm in radius in a volume of 1 cm^3.

Atmos. Chem. Phys. Discuss., doi:10.5194/acp-2016-922, 2016
Manuscript under review for journal Atmos. Chem. Phys.
Published: 29 November 2016

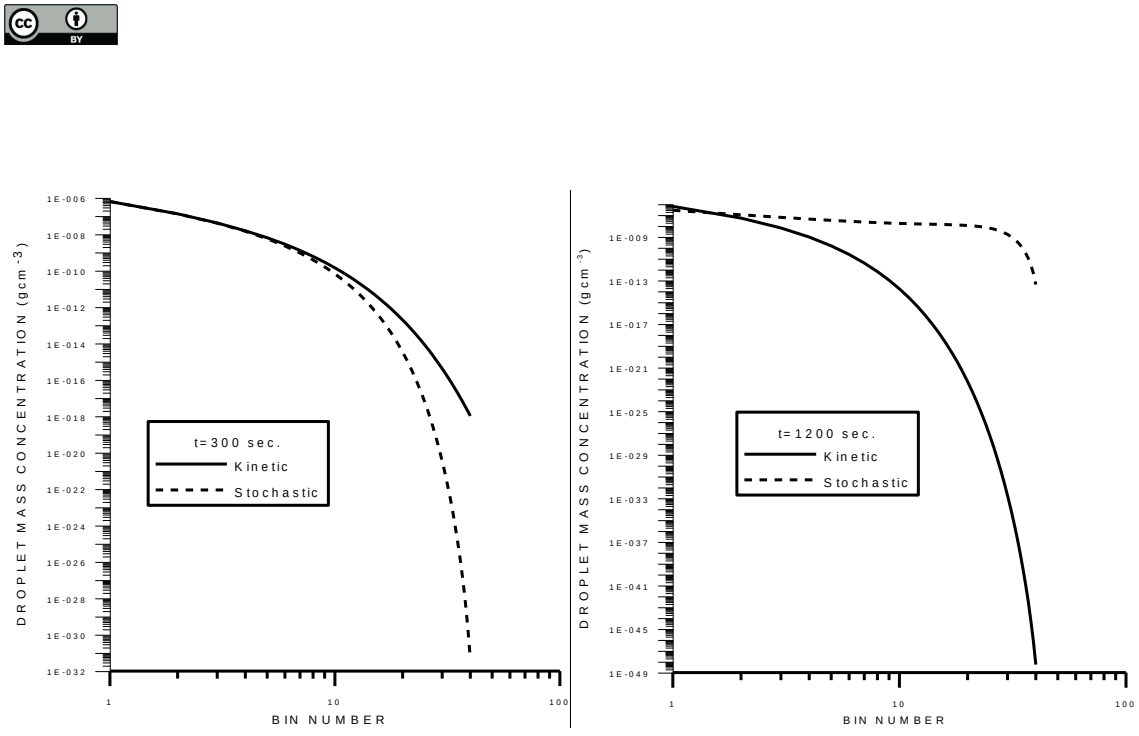

460 **(a)** **(b)**

FIG 5. Size distributions obtained from the stochastic master equation (dashed lines) and the KCE (solid lines) at: a) t=300s and b) t=1200s. Simulations were performed with the collection kernel $K(i, j) = Cx_i x_j$ (with C= 5.49x10^{10} cm^3 g^{-2} s^{-1}). The initial number of droplets was set equal to N=40 droplets of 17 μm 465 in radius in a volume of 1 cm^3. For the large end, the stochastic approach show larger values of the drop mass concentration after the sol-gel transition.

470

Atmos. Chem. Phys. Discuss., doi:10.5194/acp-2016-922, 2016
Manuscript under review for journal Atmos. Chem. Phys.
Published: 29 November 2016

475

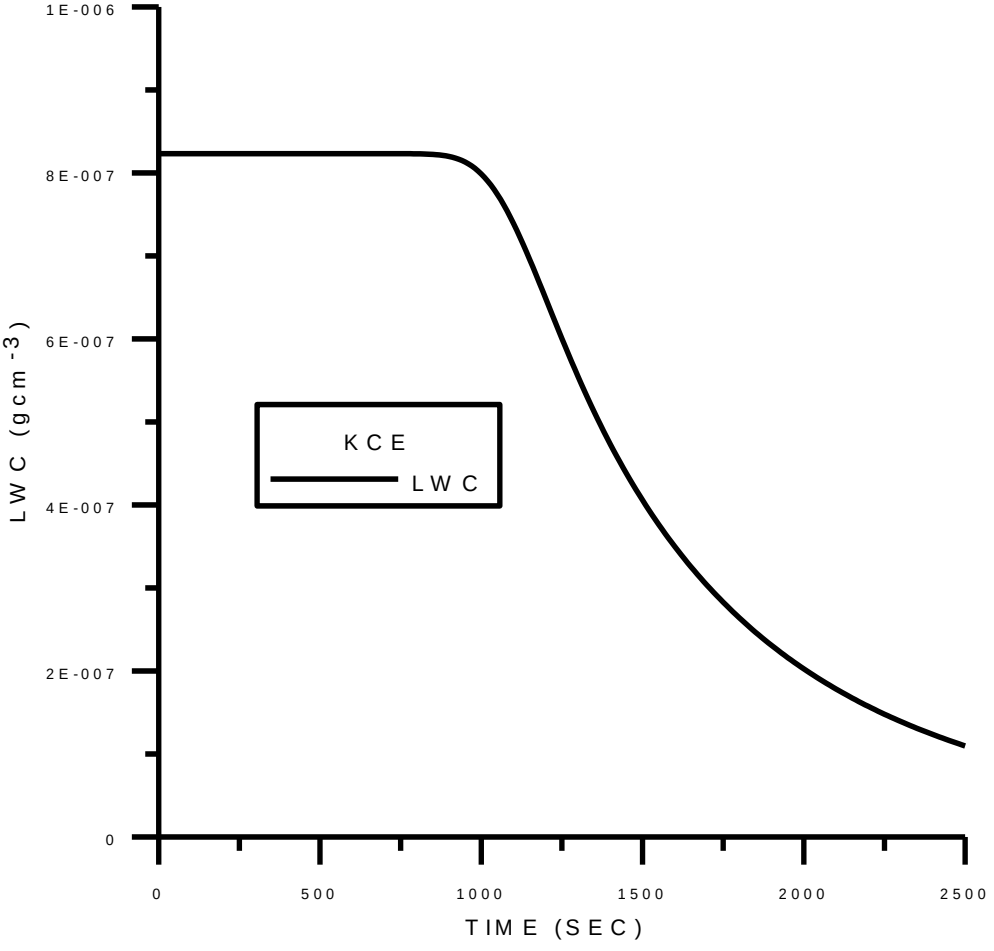

FIG 6. Time evolution of the total liquid water content calculated from the analytical solution of the kinetic collection equation for the product kernel.

480

Atmos. Chem. Phys. Discuss., doi:10.5194/acp-2016-922, 2016
Manuscript under review for journal Atmos. Chem. Phys.
Published: 29 November 2016

Atmospheric Chemistry and Physics Discussions

485

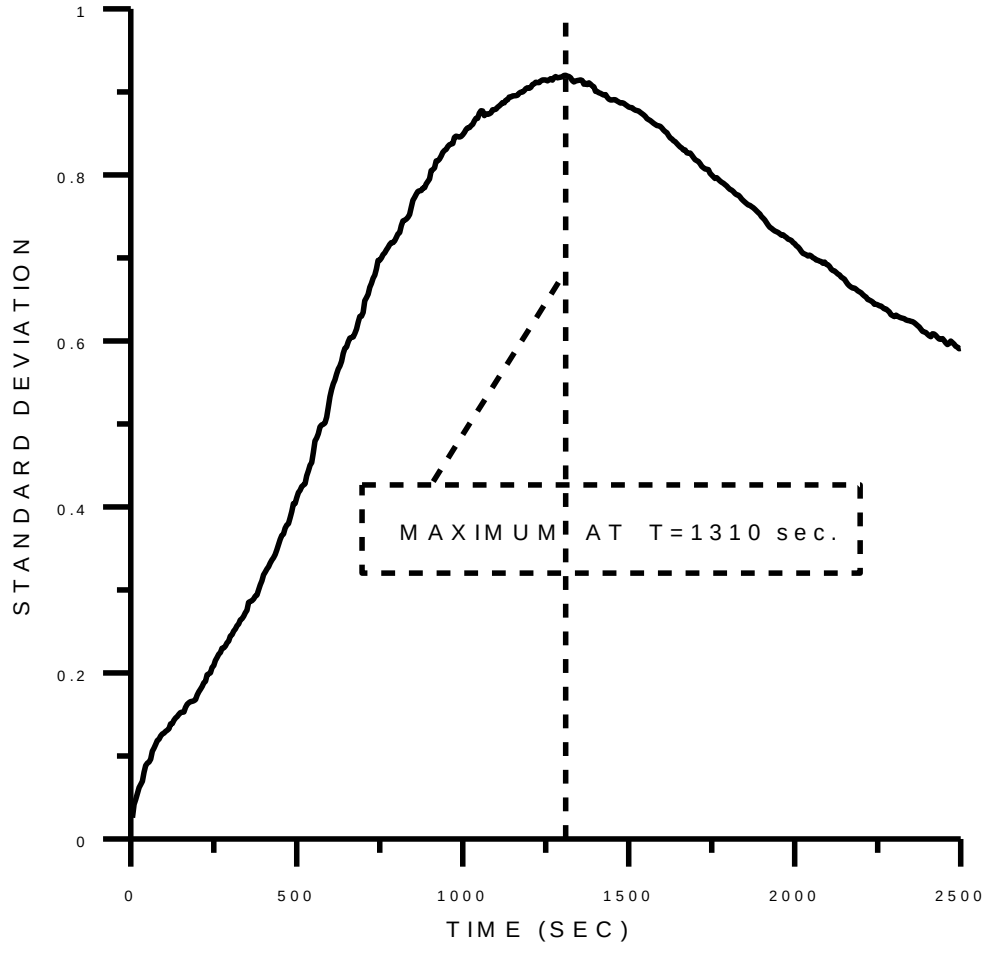

FIG 7. Time evolution of the standard deviation $\sigma(S_{max})$ of the mass of the largest droplet, for a finite system modeled with the hydrodynamic collection kernel. The initial distribution was bi-disperse with 20 droplets of 17 μm in radius and 10 droplets of 21.4 μm in a volume of 1 cm^3. The maximum of $\sigma(S_{max})$ was found at 1310 s.

490

Atmos. Chem. Phys. Discuss., doi:10.5194/acp-2016-922, 2016
Manuscript under review for journal Atmos. Chem. Phys.
Published: 29 November 2016

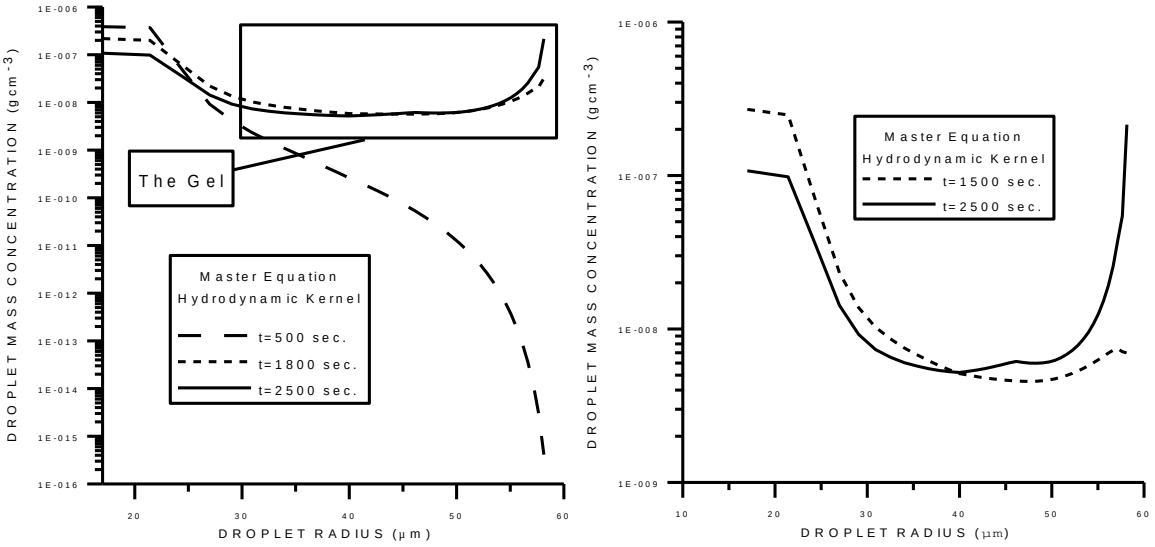

FIG 8. The droplet mass spectrum at different times (t=500, 1500, 1800 and 2500s) for a finite system modeled with the hydrodynamic collection kernel. The initial distribution is bi-disperse with 20 droplets of 17 μm in radius and 10 droplets of 21.4 μm in a volume of 1 cm^3.

Atmos. Chem. Phys. Discuss., doi:10.5194/acp-2016-922, 2016
Manuscript under review for journal Atmos. Chem. Phys.
Published: 29 November 2016

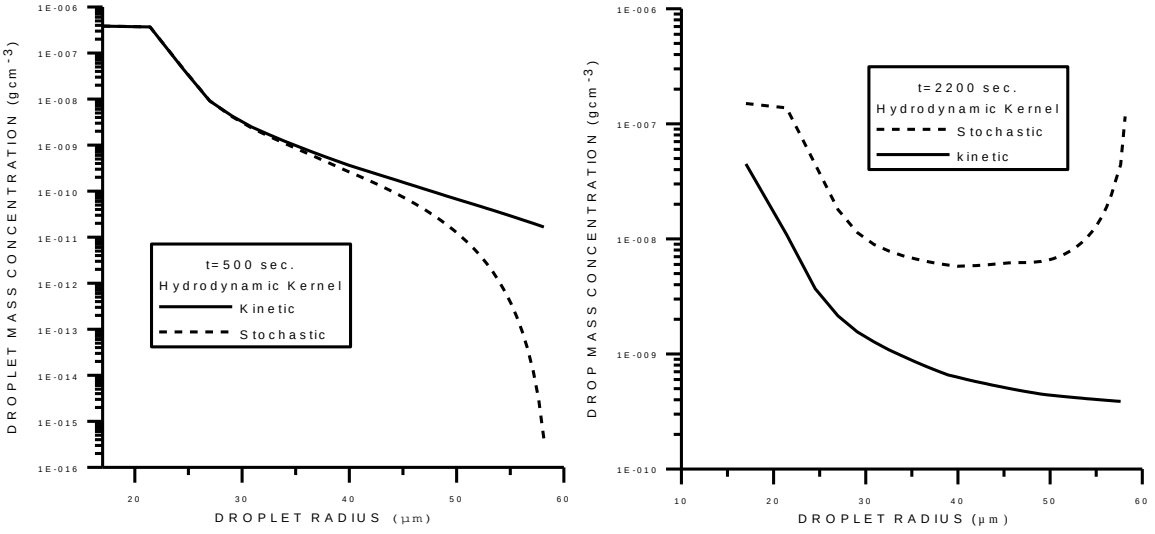

FIG 9. Comparison of the size distributions obtained from the stochastic master equation (dashed lines) with that to the KCE (solid lines) at t=500 s (in figure (a) and t=2200 s (in figure (b)) for the hydrodynamic kernel. The initial distribution was bi-disperse with 20 droplets of 17 μm in radius and 10 droplets of 21.4 μm in a volume of 1 cm^3.

Atmos. Chem. Phys. Discuss., doi:10.5194/acp-2016-922, 2016
Manuscript under review for journal Atmos. Chem. Phys.
Published: 29 November 2016

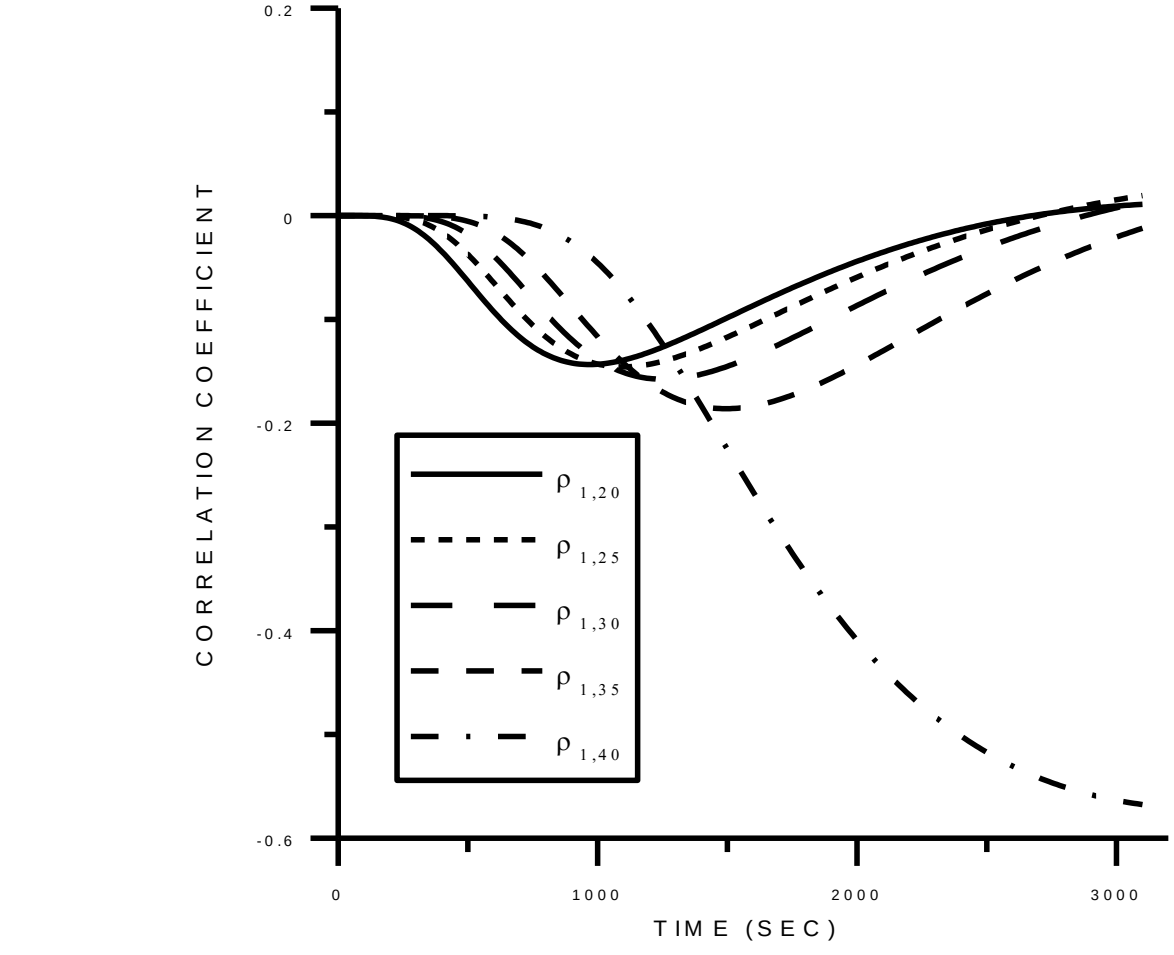

FIG. 10. Time evolution of the correlation coefficients for a $1cm^3$ system modeled with the hydrodynamic kernel, and containing initially 20 droplets of 17 μm and 10 droplets of 21.4 μm.